OPEN ACCESS

Original research

X-linked variations in *SHROOM4* are implicated in congenital anomalies of the urinary tract and the anorectal, cardiovascular and central nervous systems

Caroline M Kolvenbach,[1,2] Tim Felger,[1] Luca Schierbaum,[3] Isabelle Thiffault,[4] Tomi Pastinen,[4] Maria Szczepańska,[5] Marcin Zaniew,[6] Piotr Adamczyk,[7] Allan Bayat,[8,9] Öznur Yilmaz,[1] Tobias T Lindenberg,[1] Holger Thiele,[10] Friedhelm Hildebrandt ,[2] Katrin Hinderhofer,[11] Ute Moog,[11] Alina C Hilger,[12,13] Bonnie Sullivan,[14] Lauren Bartik,[14] Piotr Gnyś,[15] Phillip Grote,[16,17] Benjamin Odermatt,[1] Heiko M Reutter ,[18] Gabriel C Dworschak [1,3,19]

► Additional supplemental material is published online only. To view, please visit the journal online (http://dx.doi.org/10.1136/jmg-2022-108738).

For numbered affiliations see end of article.

Correspondence to
Dr Gabriel C Dworschak, Department of Neuropediatrics, University Hospital Bonn, Bonn, Germany; gabriel.dworschak@uni-bonn.de

HMR and GCD contributed equally.

Received 30 May 2022
Accepted 1 October 2022
Published Online First 15 November 2022

Check for updates

To cite: Kolvenbach CM, Felger T, Schierbaum L, *et al*. *J Med Genet* 2023;**60**:587–596.

ABSTRACT

Background *SHROOM4* is thought to play an important role in cytoskeletal modification and development of the early nervous system. Previously, single-nucleotide variants (SNVs) or copy number variations (CNVs) in *SHROOM4* have been associated with the neurodevelopmental disorder Stocco dos Santos syndrome, but not with congenital anomalies of the urinary tract and the visceral or the cardiovascular system.

Methods Here, exome sequencing and CNV analyses besides expression studies in zebrafish and mouse and *knockdown* (KD) experiments using a splice blocking morpholino in zebrafish were performed to study the role of *SHROOM4* during embryonic development.

Results In this study, we identified putative disease-causing SNVs and CNVs in *SHROOM4* in six individuals from four families with congenital anomalies of the urinary tract and the anorectal, cardiovascular and central nervous systems (CNS). Embryonic mouse and zebrafish expression studies showed *Shroom4* expression in the upper and lower urinary tract, the developing cloaca, the heart and the cerebral CNS. KD studies in zebrafish larvae revealed pronephric cysts, anomalies of the cloaca and the heart, decreased eye-to-head ratio and higher mortality compared with controls. These phenotypes could be rescued by co-injection of human wild-type *SHROOM4* mRNA and morpholino.

Conclusion The identified SNVs and CNVs in affected individuals with congenital anomalies of the urinary tract, the anorectal, the cardiovascular and the central nervous systems, and subsequent embryonic mouse and zebrafish studies suggest *SHROOM4* as a developmental gene for different organ systems.

WHAT IS ALREADY KNOWN ON THIS TOPIC

⇒ So far, missense variants or structural changes of the *SHROOM4* gene have been associated with Stocco dos Santos syndrome, a neurodevelopmental disorder, but not with congenital anomalies of the urinary tract and the visceral or cardiovascular systems.

WHAT THIS STUDY ADDS

⇒ Here, exome sequencing and copy number variation analyses identified single-nucleotide variants and microdeletions in *SHROOM4* in six affected individuals from four families presenting with congenital anomalies of the urinary tract and the anorectal, cardiovascular and central nervous systems. Embryonic mouse and zebrafish studies support a role of *Shroom4* in the development of the respective organ systems. The observed phenotypes in zebrafish following Shroom4 *knockdown* resemble the human phenotype.

HOW THIS STUDY MIGHT AFFECT RESEARCH, PRACTICE OR POLICY

⇒ The present study expands the previous knowledge on the neurodevelopmental influence of *SHROOM4* and suggests *SHROOM4* to further play an important role in the development of the urinary tract and the anorectal and cardiovascular systems.

INTRODUCTION

SHROOM4, coding for Shroom Family Member 4, is a member of the Shroom protein family that contains a N-terminal PDZ domain, a coiled coil and a C-terminal ASD2 motif (figure 1A).[1 2] Based on the domain structure, SHROOM4 protein may regulate the actin cytoskeletal architecture, which is critical for cell organisation during embryonic development.[2] A wide range of cells show expression of *Shroom4* during murine development, including the epithelium of the neural tube and kidney.[1 2] It is further expressed in adult and fetal mouse brain structures, suggesting its implication in neural function and development.[1 2]

So far, single-nucleotide variants (SNVs) in *SHROOM4* have been associated with Stocco dos Santos syndrome (MIM: 300434). Affected individuals show developmental delay (DD), mild-to-severe intellectual disability (ID), seizures, behavioural problems, autistic features, ataxia, short stature

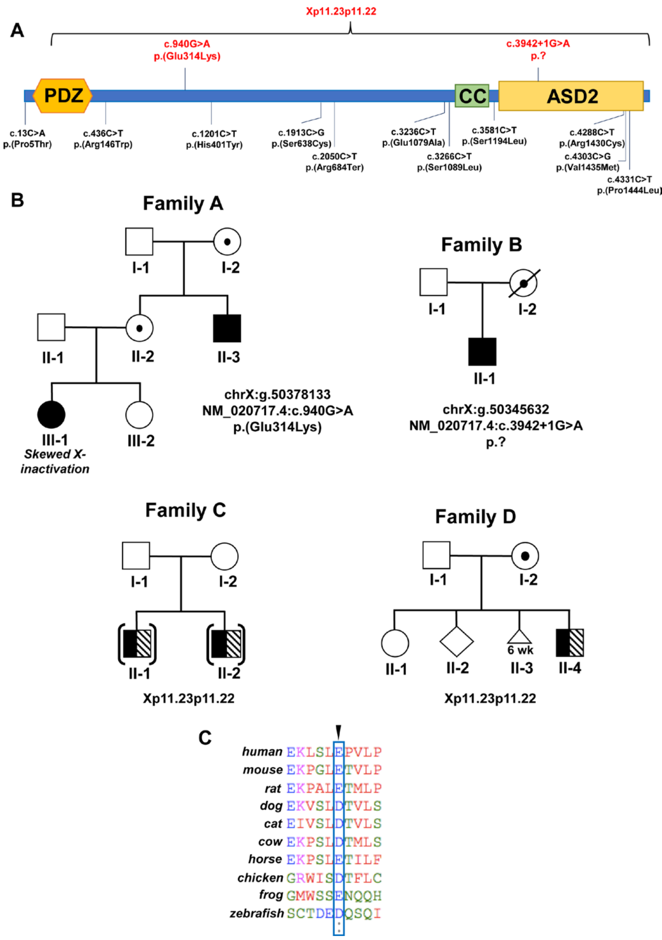

Figure 1 Exome sequencing and copy number variation analyses in families with congenital malformations identify variants in *SHROOM4*. (A) Protein domain structures are depicted (https://smart.embl.de/). The position of newly identified single-nucleotide variants of families A and B and the partial deletion of *SHROOM4* in families C and D are annotated in red. Previously reported single-nucleotide variants are shown in black. (B) Pedigree with two affected individuals in family A . III-1 presented with several congenital malformations with her maternally derived X-chromosome being activated in 84% of all lymphocytes. Pedigrees of families C and D that bear microdeletions including *CLCN5* and *SHROOM4* are depicted. Healthy carriers of variants are highlighted with a dot. Symbols representing affected individuals are shaded with different fill for differentiating clinical conditions. Black boxes depict the congenital malformation phenotype. Striped boxes illustrate Dent's disease. Brackets denote adoption. Triangle denotes miscarriage. (C) Amino acid sequence conservation among species of p.Glu314Lys that was altered in *SHROOM4* in family A. CC, coiled coil; wk, gestational age in weeks.

and skeletal abnormalities (online supplemental table S1).[3–7] Additionally, two individuals with moderate ID were found to have balanced X;autosome translocations with Xp11.2 breakpoints disrupting *SHROOM4* (online supplemental table S1).[5] Several studies using array-based comparative genomic hybridisation (CGH) in individuals with DD/ID and additional anomalies revealed microduplications, microdeletions and complex rearrangements of 0.14–8.9 Mb in size comprising chromosomal region Xp11.22 with *SHROOM4* (online supplemental table S1).[8–15] Two recent studies report seven SNVs in *SHROOM4* found in individuals with epilepsy.[16 17] Furthermore, Heide *et al*[18] found a nonsense variant in a fetus with corpus callosum agenesis. However, the phenotype of individuals with variations in *SHROOM4* remains ill-defined.

We present six individuals from four families with congenital anomalies of the urinary tract and the anorectal, cardiovascular and central nervous systems (CNS), in whom exome sequencing and copy number variation (CNV) analyses detected rare and novel SNVs in *SHROOM4*, and microdeletions comprising *SHROOM4*, respectively. Embryonic mouse and zebrafish studies suggest the additional role of *Shroom4* in the development of the urinary tract and the anorectal and cardiovascular systems, in addition to the CNS.

METHODS

Human subjects

DNA was extracted from blood or saliva. Saliva samples were collected using the Oragene DNA self-collection kit (following the Oragene DNA Purification Protocol for saliva samples).

Exome sequencing

Exome sequencing was conducted in family A. The family was previously described by Hilger *et al*.[19] For enrichment of genomic DNA, the NimbleGen SeqCap EZ HumanExome Library V.2.0 enrichment kit was used. A 100 bp paired-end read protocol on an Illumina HiSeq2000 sequencer was used. Filtering of mapped target sequences and data analysis were performed using the 'Varbank' exome analysis pipeline (https://varbank.ccg.uni-koeln.de/varbank2/) as described previously.[20] In short, variants were ranked on the basis of their probable effect on the function of the encoded protein considering evolutionary conservation among orthologues across phylogeny using ENSEMBL Genome Browser (https://www.ensembl.org/index.html) and assembled using Clustal Omega (https://www.ebi.ac.uk/Tools/msa/clustalo/), as well as the in silico prediction programmes PolyPhen-2 (http://genetics.bwh.harvard.edu/pph2/), SIFT (https://sift.bii.a-star.edu.sg/), Combined Annotation Dependent Depletion (CADD) (https://cadd.gs.washington.edu/) and MutationTaster (http://www.mutationtaster.org/). Splice site variants were evaluated using the in silico prediction tools MaxEnt (http://hollywood.mit.edu/burgelab/maxent/Xmaxentscan_scoreseq_acc.html), NNSPLICE (https://www.fruitfly.org/seq_tools/splice.html), SSF (http://www.umd.be/searchsplicesite.html) and EX-SKIP (https://ex-skip.img.cas.cz/). Variant filtering based on population frequency was performed using population database gnomAD (https://gnomad.broadinstitute.org/) to include only rare alleles (ie, minor allele frequency <1%). Remaining variants were confirmed by Sanger sequencing. The website GeneMatcher (https://genematcher.org/) enabled the connection between researchers caring for family B.[21 22]

For family B, exome libraries were prepared using the Illumina TruSeq PCR-Free library preparation kit with 10 cycles of PCR, followed by enrichment with the IDT xGen Exome Research Panel V.2, with additional spike-in oligos (Integrated DNA Technologies) to capture the mitochondrial genome and dispersed genomic regions for CNV detection. Samples were sequenced to a minimum of 7 Gb of 2×125 paired-end reads for a mean of 80× average coverage or greater on the Illumina HiSeq 4000 or Illumina NovaSeq 6000. Bidirectional sequence is assembled, aligned to reference sequences based on human genome build GRCh37/UCSC hg19 and analysed using custom-developed software, RUNES and VIKING (https://www.childrensmercy.org/childrens-mercy-research-institute/research-areas/genomic-medicine-center/data-and-software-resources/). The analysis is confined to the genes of interest for the individual and with a minor allele frequency corresponding to disease incidence.

Copy number variants

Initial diagnosis in individual II-2 (family C) was performed using genome-wide oligonucleotide microarray (SurePrint G3 ISCA V.2 8×60 k, Agilent Technologies) with a mean resolution of 60 kb. For molecular karyotyping of individuals II-1 and II-2 in family C, we used the Illumina Infinium Global Screening Array-24 V.2.0 plus multidisease add-on content BeadChip. Visualisation of deletion was performed using GenomeStudio Genotyping Module V.2.0.5 (www.illumina.com/). Array analysis in family D was performed using the SurePrint G3 ISCA V.2 8×60 k (Agilent Technologies). Detected CNVs in our study were evaluated for overlapping CNVs annotated in the Database of Genomic Variants (DGV) (http://dgv.tcag.ca) and in the DatabasE of genomiC varIation and Phenotype in Humans using Ensembl Resources (DECIPHER) (https://decipher.sanger.ac.uk/).

Skewed X-chromosome inactivation

Testing for skewed X-chromosome inactivation was performed in individuals II-2 and III-1. We determined the X-inactivation status at the CAG repeat of the first exon of androgen receptor locus *AR* (NM_000044.6). DNA was treated with methylation sensitive restriction endonuclease *Hpa*II. Treated and untreated DNAs were amplified by PCR with FAM-fluorescence labelled HUMARA primer 1 (5′-GCTGTGAAGGTTGCTGTTCCTCAT-3′) and primer 2 (5′-TCCAGAATCTGTTCCAGAGCGTGC-3′).[23] PCR products were separated on an ABI PRISM 3100 Genetic Analyzer (Thermo Fisher). The fluorescence-labelled PCR fragments were analysed with GeneMapper software (Applied Biosystems). The peak area of each fragment was quantified and compared between treated and untreated samples to determine the methylation pattern of maternally and paternally inherited X-chromosomes. Testing showed skewed X-inactivation in III-1 with her maternally derived X-chromosome being activated in 84% of all lymphocytes.

Mouse in situ hybridisation (ISH)

Mouse embryos from a wild-type (wt) SWISS background of embryonic days (E) 12.5 were dissected into PBS and fixed overnight in 4% PFA at 4°C. Embryos were processed into paraffin wax, and 5 µm sections were made using a microtome. The probe corresponds to the 3′ coding region of *Shroom4* (ENSMUSG00000068270). Two primers were used to amplify a 995 bp region from mouse embryo cDNA (forward: TTGGGGCCCGAAAGAAGGTC, reverse: TTCCCTGCCATCCACATGCT), and at the reverse primer, a T7 polymerase sequence was included. The protocol of the probe generation can be found online (http://mamep.molgen.mpg.de). In vitro transcription was performed using a nucleotide mix containing digoxigenin-11-UTP (Roche). All samples were processed for ISH as described by Chotteau-Lelièvre *et al*[24] with minor modifications, and detection of AP activity was carried out using BM Purple (Roche). Images were obtained on a Leica M205C System with a colour camera.

Zebrafish lines and maintenance

Zebrafish were kept according to national law and to recommendations by Westerfield[25] in our zebrafish facility in Bonn, Germany. Zebrafish larvae (zfl) of wt AB/TL and the transgenic *Tg(wt1b:eGFP)* reporter lines were obtained by natural spawning and were raised at 28°C in Danieau (30%) on a 14-hour light:10-hours dark cycle. All zebrafish experiments were performed at ≤5 days post fertilisation (dpf). To suppress pigmentation, 0.003% 1-phenyl-2-thiourea was added to the Danieau solution for respective zfl from 1 dpf onward. Staging was performed according to Kimmel *et al*.[26]

Whole-mount zebrafish ISH

The cDNA plasmid for the preparation of antisense and sense probes for *shroom4* was generated by PCR from zebrafish poly-T embryonic cDNA with specific primers (forward: CATCATctgcagcgatgagatctgtgagaatgagc, reverse: CATCATggatcccagctttttacgcagactctcc). The resulting PCR products were cloned into pGEM-T Easy. Constructs were linearised by corresponding restriction enzymes, and Dig-labelled RNA was synthesised using Roche Dig labelling kit. ISH was performed following the instructions of Thisse and Thisse.[27]

Microinjections of morpholino oligonucleotides (MOs) and mRNA

Embryos at the one-cell to two-cell stages were pressure injected into the yolk with a splice blocking MO synthesised by Gene-Tools, LLC. Injections were carried out with 1.27 ng of *shroom4* MO (1.8 nL/embryo) (5′-ACATTTGTGTGTTTGCTTACCTTCG-′3) and 1.27 ng of standard control (Ctrl) MO (5′-CCTCTTACCTCAGTTACAATTTATA-′3) that targets transcripts *shroom4-201* (ENSDART00000111542.5) and *shroom4-202* (ENSDART00000170100.3). For human mRNA rescue experiments, 75 pg of in vitro transcribed human *SHROOM4* mRNA was injected into the yolk of one-cell embryos. *SHROOM4* mRNA was transcribed from cDNA clone H06D041O16 (Source BioScience) containing NM_020717.4 using the mMESSAGE Machine T7 Kit (Ambion 1340M) and the Poly (A) Tailing Kit (Ambion AM1350).

Western blot analysis

Zfl were pooled into samples of 20–30 and lysed in RIPA buffer on ice with 4% protease inhibitor using a sonicator. Protein sample (50 µg) was separated by sodium dodecyl-sulfate polyacrylamide gel electrphoresis (SDS-PAGE), transferred on PVDF membranes and probed with a custom made anti-Shroom4 antibody (1:1000; polyclonal, rabbit AB2501, anti Aa 550–565, C-SERFATNLRNEIQRKK; Thermo Fisher Scientific) at 4°C overnight.

Sulforhodamine 101 (SR101) excretion assay

Excretion assay with 0.02 mM SR101 was performed on 5 dpf as previously described by our group.[28]

Eye-to-head ratio

Zfl were phenotyped at 4 dpf using a ZEISS Stemi508 for brightfield imaging. The time point of 4 dpf was chosen since the phenotype was most prominent. The diameters of the eyes were measured with NIS-Element Viewer software. To account for variation and growth effects, eye size was normalised to head (snout to otic vesicle).[29] Zfl were anaesthetised with 0.03% tricaine and fixed in 1.25% low-melting agarose for imaging.

Phalloidin stainings

Phalloidin stainings were performed according to previous reports.[30 31] *shroom4* MO-injected zfl were fixed at 5 dpf in 4% PFA overnight at 4°C and subsequently washed three times for 5 min in phosphate-buffered saline (PBS) with 0.1% Tween-20

(PBST) and 5 min in PBS-Tx (2% Triton X-100). Afterwards, zfl were incubated for 2 hours in PBS-Tx to allow permeabilisation. Stainings with 2 µg/mL tetramethyl rhodamine B isothiocyanate (Sigma Aldrich, P1951) were conducted overnight at 4°C. Stained zfl were briefly washed in PBS before applying DAPI (ACDBio, RNAscope DAPI, 320858) overnight at 4°C. Zfl were washed in PBS before imaging.

Imaging

At the stages of interest embryos were analysed under a Nikon AZ100 Macro-Zoom microscope. Selected embryos were anaesthetised with 0.016% tricaine, fixed in 2% low-melting agarose and imaged by two-photon scanning fluorescence in vivo microscope (LaVision Trim-ScopeII, Imspector and ImageJ software).

Statistical analysis

Two-tailed Student's t-test, Mantel-Cox and two-way analysis of variance test were used for analysis using GraphPad Prism V.6. Differences with a p value of <0.05 (*) were considered as being statistically significant.

RESULTS

Exome sequencing identifies rare variants in *SHROOM4*

In family A, the index individual (III-1) and her maternal uncle (II-3) showed four major component features (CFs) of the VATER/VACTERL association (MIM: 192350) (figure 1B and table 1; for detailed information, see online supplemental Note). An initial CNV analysis did not detect any disease-causing CNV in III-1, II-2 and II-3 of family A.[19] Skewed X-chromosome inactivation testing in the index individual (III-1) and her mother (II-2) demonstrated skewing of the X-chromosome bearing the

Table 1 Genetic and phenotypical overview of affected individuals with changes in *SHROOM4*

Family	Family A		Family B		Family C		Family D
Individual	III-1	II-3	II-1		II-1	II-2	II-4
Sex	Female	Male	Male		Male	Male	Male
Chr. position (hg19)	chrX:g.50378133	chrX:g.50378133	chrX:g.50345632		Xp11.23p11.22	Xp11.23p11.22	Xp11.23p11.22
Inheritance	Maternally inherited (skewed X chr)	Maternally inherited	Maternally inherited		Parents not available for testing	Parents not available for testing	Maternally inherited
Nucleotide change	NM_020717.4: c.940G>A	NM_020717.4: c.940G>A	NM_020717.4: c.3942+1G>A	**Type**	Deletion	Deletion	Deletion
Amino acid change	p.(Glu314Lys)	p.(Glu314Lys)	p.?	**Minimal region affected**	chrX:g.49,369,600–50,447,320	chrX:g.49,369,600–50,447,320	chrX:g.49,375,617–52,838,206
CADD	20.5	20.5	NA	**Size**	1.07 Mb	1.07 Mb	3.46 Mb
gnomAD allele frequencies (hom/hemi/het/wt)	0/0/1/178,700	0/0/1/178,700	Not reported				
Renal and GU	Unilateral renal agenesis	Unilateral renal agenesis	Renal dysplasia and micropenis		PUV, cryptorchidism, proteinuria, hypercalciuria and nephrocalcinosis (Dent's disease)	PUV, proteinuria and nephrocalcinosis (Dent's disease)	PUV, bilateral hydronephrosis, renal cortical microcyst, micropenis, cryptorchidism, proteinuria and hypercalciuria (Dent's disease)
Neurological development			Hypotonia		DD and intellectual disability	DD, delayed speech and intraventricular bleeding	DD, increased muscular tone of lower limbs and epilepsy
Gastrointestinal	EA with fistula (Vogt type 3b)	EA with fistula (Vogt type 3b)	Gastric reflux and failure to thrive			Failure to thrive	Failure to thrive
Anorectal	ARM with vestibular fistula	ARM					
Cardiac		Tetralogy of Fallot	ASD and persistent foramen ovale				
Skeletal		Aplasia of right radius bone and left preaxial polydactyly	Clinodactyly of the fifth finger and equinovarus		Short stature	Short stature and extremeties	
Craniofacial features			Overfolded helix, depressed nasal bridge, highly arched eyebrow, hypertelorism, micrognathia and posteriorly rotated ears			Prominent frontal tumours, depressed nasal bridge, hypertelorism, high arched palate and retinal thinning	Protruding eyes
Skin and hair			Mongolian blue spot and single transverse palmar creases			Atopic skin, oedema of the dorsal parts of the feet and lower legs, and periodic red colour of oedematous skin	Single transverse palmar crease
Endocrine					Hypothyreosis		
Immune						Low C3/C4 and low immunoglobulins	Low C3/C4 and low immunoglobulins
Electrolytes						Hypomagnesaemia, hyponatraemia, hypophosphataemia, hypokalaemia, hypokalcaemia and hypochloremia	Hypophosphataemia
Other			Single umbilical artery, nuchal cord and sacral dimple		Fanconi syndrome, suspected shaken baby syndrome with subdural hygroma and retinal bleeding		Retinitis pigmentosa, omphalocele and inguinal hernia

ARM, anorectal malformation; ASD, atrial septal defect; CADD, Combined Annotation Dependent Depletion; chr, chromosome; DD, developmental delay; EA, oesophageal atresia; GU, genitourinary; hemi, hemizygous; het, heterozygous; hom, homozygous; Mb, megabase; NA, not applicable; PUV, posterior urethral valve; wt, wild type.

wt allele in III-1 with her maternally derived X-chromosome being activated in 84% of all lymphocytes tested (figure 1B and table 1). Successive exome analysis prioritising X-chromosomal variants revealed a rare variant in *SHROOM4* (NM_020717.4), detected in the affected individuals II-3 and III-1 and in the conducting mother (II-2) and maternal grandmother (I-2) (NM_020717.4:c.940G>A p.(Glu314Lys), ClinVar: SCV002498760), but not in the other family members I-1, II-1 and III-2 (figure 1A,B, and table 1). The p.(Glu314) glutamate is conserved among vertebrates down to *Xenopus tropicalis* (figure 1C). Other vertebrates exhibit the amino acid aspartate, also acidic, at this respective position. Three out of four in silico prediction programmes rate the amino acid change as potentially damaging (CADD: 20.5, MutationTaster: disease causing, SIFT: deleterious, PolyPhen-2: 0.003 (benign)). One heterozygous female carrier in 178 700 alleles (allele frequency 0.000005596) for this variant has been reported in the gnomAD online database (table 1). The variant does not reside in one of the two known functional protein domains (figure 1A). According to the standards and guidelines for the interpretation of sequence variants of the American College of Medical Genetics and Genomics (ACMG), we rated this variant as variant of uncertain significance (VUS).

Using the online tool GeneMatcher, we identified another male individual (family B, II-1) presenting with a sacral dimple, atrial septal defect, unilateral kidney dysplasia, bilateral clinodactyly of the fifth finger, left-sided single palmar crease and pes equinovarus (table 1).[21 22] Additionally, he showed dysmorphic craniofacial features, gastro-oesophageal reflux, hypotonia and failure to thrive (table 1). A hemizygous novel splice site variant in *SHROOM4* was identified by exome sequencing (NM_020717.4:c.3942+1G>A, ClinVar: SCV002498761), not reported in gnomAD (figure 1B and table 1). The variant resides in the essential splice-donor site, likely causing retention of intronic DNA or splicing out of exons, possibly disrupting the ASD2 motif (figure 1A).[2 32] Four in silico splicing programmes (MaxEnt, NNSPLICE, SSF and EX-SKIP) predict that the nucleotide change has a 100% impact on splicing. The variant was maternally inherited (I-2) (figure 1B and table 1). The mother had a medical history of depression and seizures; furthermore, her medical history describes a cardiomegaly of unknown origin with medical reports lacking. The mother died in the first year of the child's life. The variant was rated as VUS according to the ACMG guidelines.

Microdeletion Xp11.23p11.22 with loss of *SHROOM4* and *CLCN5*

Individual II-1 from family C presented with congenital anomalies and neurocognitive impairment (figure 1B and table 1). He showed DD, later ID, short stature, posterior urethral valves (PUVs) and clinical characteristics of Dent's disease. Based on the findings of subdural hygroma and retinal bleeding, shaken baby syndrome was suspected. His younger brother, II-2, presented with dysmorphic craniofacial features, DD, intraventricular haemorrhage, short stature, short limbs, failure to thrive, PUV and Dent's disease (table 1). Array CGH analysis in individual II-2 identified a 1.07 Mb microdeletion at Xp11.23p11.22 spanning chrX:g.49,375,617–50,447,320 (hg19) (ClinVar: SCV002498762). The deletion involves eight coding genes (*PAGE1*, *PAGE4*, *USP27X*, *CLCN5*, *AKAP4*, *CCNB3*, *DGKK* and partially *SHROOM4* (8 of 9 exons deleted, NG_011882.1)), and six microRNAs (figure 1A and online supplemental figure S1). SNP array analysis confirmed the deletion of individual II-2 and showed the same deletion in individual II-1 (figure 1B and online supplemental figure S1). Combining both array data, we were able to refine the breakpoints to chrX:g.49,369,600–50,447,320, with the 3′ breakpoint residing within chrX:g.49,174,104–49,369,600 and the 5′ breakpoint residing within chrX:g.50,447,320–50,450,462. Parental DNA for segregation analysis was not available since both brothers were adopted, with the biological parents being lost to follow-up.

Individual II-4 from family D presented with congenital anomalies and neurocognitive impairment (figure 1B and table 1). He showed DD, increased muscular tone of the lower limbs, protruding eyes, retinitis pigmentosa, PUV, bilateral hydronephrosis, renal cortical microcysts, omphalocele, micropenis, cryptorchidism, inguinal hernia, unilateral single transverse palmar crease and clinical characteristics of Dent's disease. The boy was the third born child to unrelated parents. The course of pregnancy was complicated by gestational diabetes, arterial hypertension and Grave's disease. The oldest sister, II-1, is healthy (figure 1B). Individual II-2 was unavailable for clinical evaluation and genetic testing. The mother had a spontaneous miscarriage (II-3) at 6 weeks of gestation (figure 1B). Array CGH analysis in the affected individual, II-4, identified a 3.46 Mb microdeletion at Xp11.23p11.22 comprising chrX:g.49,375,617–52,838,206 (hg19) (ClinVar: SCV002498763) (figure 1A). This microdeletion was maternally inherited.

In accordance with the ACMG standards and guidelines for interpretation and reporting of postnatal constitutional CNVs, identified microdeletions in families C and D were rated as CNVs of uncertain clinical significance. We did not detect any relevant overlap with CNVs annotated in DGV. However, there was one individual annotated in DECIPHER with a 382 kb maternally inherited hemizygous deletion covering the first exon and a large proportion of intron 1 of *SHROOM4*.[33] This individual (434791) was noted to have global DD. Other entries comprising very large (>50 Mb) deletions or entries lacking phenotype information were considered as not relevant.

Expression of *Shroom4*/*shroom4* in murine embryos and zfl

To study the expression of the canonical *Shroom4* transcript (ENSMUST00000103005.10) in mouse embryos, we performed ISH studies, which showed expression in the brain and other neuronal tissues, vertebrae and genital tubercle at E12.5 (figure 2A,B). In order to further investigate the function of *SHROOM4* during organ development, we used zebrafish as a model organism. BLAST analysis with human *SHROOM4* identified a single zebrafish *shroom4* orthologue (ENSDARG00000079900). To study the expression of *shroom4* in zfl, we generated a labelled antisense RNA probe for ISH. In accordance with previous work, we detected strong expression of *shroom4* in the head, brain, eyes, heart, pectoral fins, the intestine and cloacal region at 48 hours post fertilisation (hpf) (figure 2C–E) and 72 hpf (data not shown).[34]

Knockdown (KD) of Shroom4 leads to reduced survival, pericardial effusion (PE), glomerular cysts, abnormal eye-to-head ratio and cloacal anomalies

The similarity of the amino acid sequences between the human SHROOM4 and zebrafish Shroom4 proteins amounts to 73%. In order to study the phenotypical effect of a Shroom4 depletion in zebrafish, we applied a KD with a splice blocking MO that targets both existing transcripts, *shroom4-201* (ENSDART00000111542.5) and *shroom4-202*

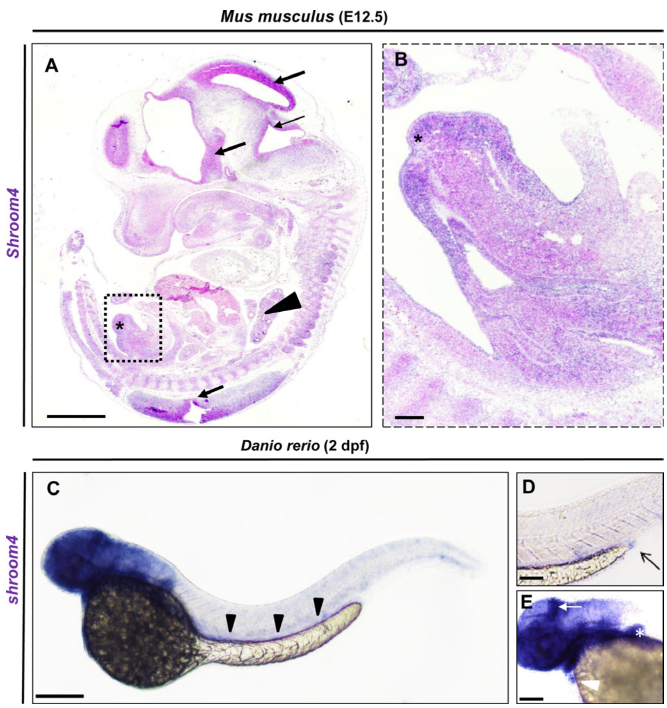

Figure 2 *Shroom4/shroom4* is expressed during early mouse and zebrafish development. (A,B) ISH with *Shroom4* probe on a sagittal section of a representative E12.5 (TS21) *Mus musculus*. *Shroom4* expression is visible (in blue) in the head and neuronal tissues (black arrows), Vertebrae (black arrowhead), and genital tubercle (asterisks). Magnification (square in A) highlights the expression in the developing genitourinary tract (B). (C) Whole-mount ISH with an anti-*shroom4* probe shows the expression of *shroom4* RNA (in blue) at 2 days post fertilisation in the head, brain, eyes, fins, heart, the intestine (black arrowheads) and cloacal region in *Danio rerio*. Sense controls did not show a staining (not shown). (D) The cloaca is highlighted by an arrow in the enlargement. (E) The expression of *shroom4* is highlighted by a white arrow in the brain and by a white arrowhead in the heart in the enlargement. Positive expression in the pectoral fins is marked by the white asterisk. Scale bars represent 1 mm (A), 10 µm (B) and 100 µm (C). ISH. In situ hybridisation.

(ENSDART00000170100.3) (online supplemental figure S2A). Efficiency of MO-induced KD was demonstrated by RT-PCR with a decrease of wt *shroom4* expression and presence of an alternative band without exon 2 for transcript *shroom4-201* (online supplemental figure S2B-C). Similarly, RT-PCR for transcript *shroom4-202* confirmed efficiency, showing an insertion of 41 intronic bp (online supplemental figure S2B,C). No change in *eef1a1* (ENSDARG00000039502) expression was detected, serving as Ctrl (online supplemental figure S2C). Western blot analysis confirmed these findings on the protein level (figure 3A). Following the KD of Shroom4, we observed reduced survival of the MO-injected zfl (26%) compared with Ctrl MO-injected zfl (76%) at 5 dpf (figure 3B). Furthermore, MO-injected zfl displayed short body length, PE, a reduced eye and head size (eye-to-head ratio), as well as glomerular cysts and pronephric dilatation (figure 3C–H). PE was found in 71% of *shroom4* morphants but only in 13% of Ctrl larvae (figure 3C,D). The measured eye size was normalised to head length to account for variation in embryo size (figure 3E). This ratio was significantly lower in *shroom4* MO zfl (0.37) compared with Ctrls (0.46) (figure 3F). To assess the impact of the Shroom4 KD on the kidneys and urinary tract, we used the transgenic *Tg(wt1b:eGFP)* fluorescent reporter line, expressing GFP in the kidney during development (figure 3G,H).[35] We observed the occurrence of glomerular cysts and dilatation of the pronephric ducts at 2 dpf in 52% of with MO-injected zfl but only in 13% of Ctrls (figure 3G,H). Rescue experiments that were conducted by coinjection of human wt *SHROOM4* mRNA together with *shroom4* MO resulted in statistically significant increased survival (58%) (figure 3B). The observed phenotype PE in MO-injected zfl could be rescued (MO+wt RNA: 51%) (figure 3C). The reduced eye size and head length could also be rescued by coinjection with human wt *SHROOM4* mRNA to a ratio of 0.42 (figure 3F). Nevertheless, the occurrence of glomerular cysts and pronephric dilatation could not be rescued (47%) (figure 3G). Overexpression of human wt *SHROOM4* mRNA did not cause increased mortality or any phenotypical changes (figure 3B,C,F,G).

On the analogy of the observed anorectal phenotypes in family A, we were interested in studying the impact of Shroom4 depletion on cloacal development in zfl. Therefore, we applied phalloidin stainings that mark actin filaments and allow visualisation of zebrafish cloacal morphology.[30 31] In comparison with Ctrls, the *shroom4* MO-injected zfl exhibited a distension of the hindgut and dilated distal pronephric ducts, potentially due to distal obstruction caused by cloacal malformation (figure 4A,B). Next, we performed an SR101 excretion assay to confirm the potential hindgut anomalies in MO KD zfl. Zfl ingest SR101, a red fluorescent dye labelling the intestine, which enables examination of the opening of the cloaca and ensuing excretion of SR101 at 5 dpf. *shroom4* MO-injected zfl showed a significantly prolonged time to excretion and fewer numbers of excretion (figure 4C–F). In addition, no or just oscillating peristalsis was observed in *shroom4* morphants in contrast to Ctrls that all showed regular peristalsis of the intestine (figure 4G). These assays demonstrate the high abundance of cloacal opening defects in *shroom4* morphants resembling the anorectal phenotype in humans.

DISCUSSION

Previously, variations in *SHROOM4* have been associated with Stocco dos Santos syndrome (MIM: 300434), a neurodevelopmental disorder (online supplemental table S1).[3–15 36] Here, we identified genetic variations of different size affecting *SHROOM4* in individuals with multiple congenital anomalies of the urinary tract, the anorectal and cardiovascular systems, and the CNS. The respective individuals presented with overlapping phenotypical features, including congenital anomalies of the urinary tract system (6/6), the CNS (4/6), the anorectum (2/6) and the cardiovascular system (2/6) (table 1). The two affected individuals of family A fulfil the clinical criteria of VATER/VACTERL association, defined by the presence of at least three of the following CFs: vertebral anomalies (V), anorectal malformations (A), cardiac defects (C), tracheo-oesophageal fistula and/or oesophageal atresia (TE), renal anomalies (R) and limb anomalies (L).[19] Previously described affected individuals with ID and DD carrying variations in *SHROOM4* presented with features that concern anatomical structures affected by the VATER/VACTERL spectrum (online supplemental table S1).[3–6 10–14] These comprised the heart in one individual, kyphosis and scoliosis, small hands, small feet, camptodactyly and clinodactyly (online supplemental table S1). Nevertheless, kyphosis and scoliosis may be secondary to a neurogenic genesis, and the described limb anomalies are observed in other syndromes and are not specific for VATER/VACTERL association (ie, small hands and feet).

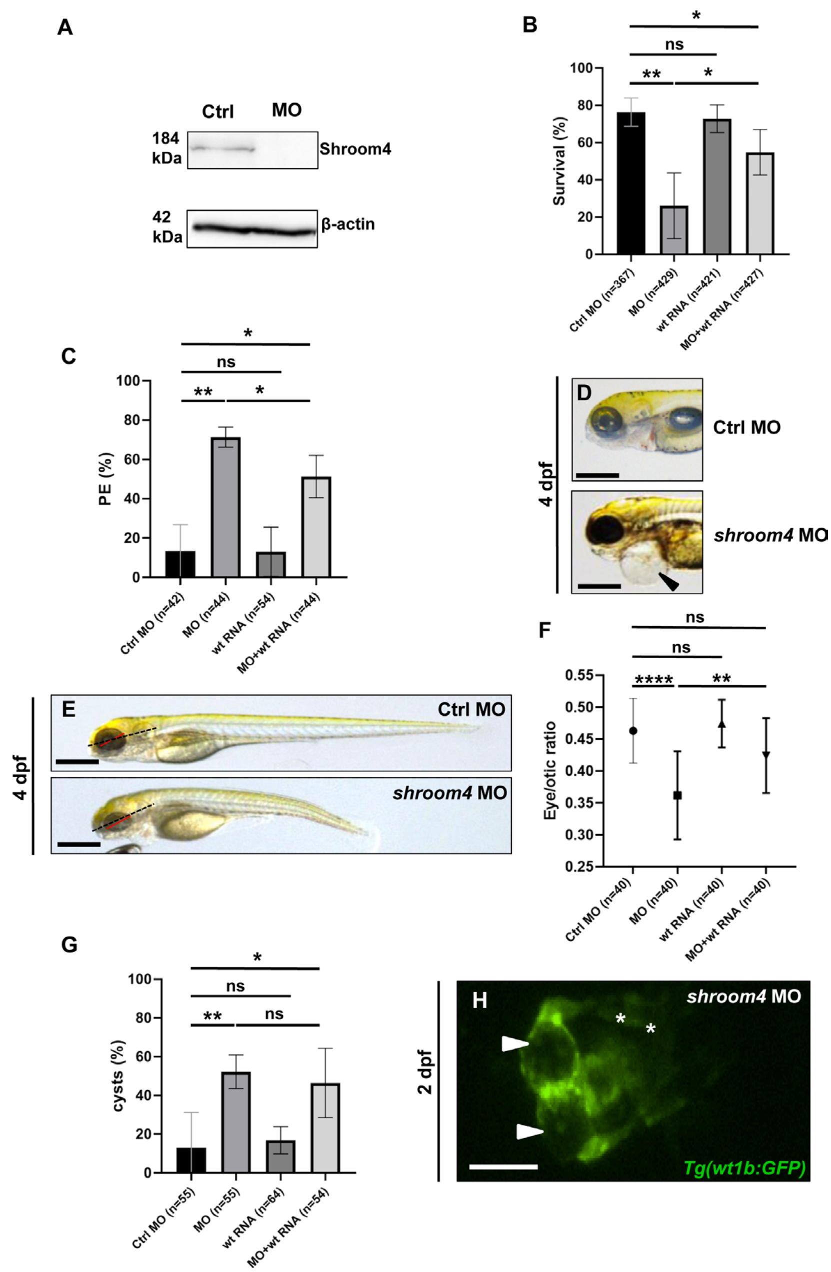

Figure 3 *Knockdown* of Shroom4 leads to glomerular cysts, eye abnormalities and PE. (A) Western blot analysis demonstrates a protein decrease in *shroom4* MO-injected zfl for Shroom4 (184 kDa, F1Q6C1), derived from transcript *shroom4-201*, in comparison with Ctrl MO-injected zfl. The protein product for transcript *shroom4-202* is too small to be detected by Western blot analysis (11 kDa, B3DGK9). β-Actin serves as Ctrl and shows an equal amount of protein in both samples. (B) Quantification of survival (n=5); zfl injected with *shroom4* MO show a significant reduction of survival rate at 5 dpf compared with Ctrl MO. Survival of *shroom4* MO is significantly rescued by coinjection of human WT *SHROOM4* RNA. No alterations in survival have been observed by solely injecting WT *SHROOM4* RNA. (C,D) Quantification of PE (n=3) shows significant occurrence in *shroom4* morphants, a phenotype, which could be rescued by co-njection of WT *SHROOM4* RNA. Black arrowhead highlights PE observed in a zfl injected with *shroom4* MO at 4 dpf. (E,F) Eye-to-head ratio of injected zfl at 4 dpf (n=4). Measurement of the eye (red line) and head (black line, distance between the snout to the otic vesicle) was performed as visualised (F). Injection of *shroom4* MO significantly reduced eye-to-head ratio, while WT mRNA co-injection in *shroom4* MO-injected zfl significantly rescues the phenotypical effect. (G,H) Zfl injected with *shroom4* MO develop glomerular cysts (white arrowheads in H) and dilatation of the pronephric ducts (white asterisks in H) that could not be rescued by human WT RNA (n=4). Images from in vivo observation through fluorescence microscopy (dorsal view) in *Tg(wt1b:GFP)* were taken at 2 dpf. Scale bars represent 100 µm. Ctrl, control; MO, morpholino oligonucleotide; ns, nonsignificant; PE, pericardial effusion; wt, wild type; zfl, zebrafish larvae. $p < 0.05$ (*), $p < 0.01$ (**), $p < 0.001$ (***)

Pathogenic variants in *CLCN5* are associated with Dent's disease, a renal proximal tubulopathy, characterised by proteinuria, hypercalciuria and hyperphosphaturia, kidney stones and, in some cases, kidney failure.[37] Around 8% of pathogenic variants are deletions.[38] Three of the affected individuals described here carry a deletion comprising *CLCN5*, causing the phenotype of Dent's disease. However, all three individuals presented also with PUV (3/3), an anatomical obstruction of the urethra not associated with Dent's disease. Additionally, all three individuals (3/3) show neurodevelopmental disorders, also not associated with pathogenic *CLCN5* variations. Our human genetic data suggest that the *SHROOM4* deletions may be implicated in

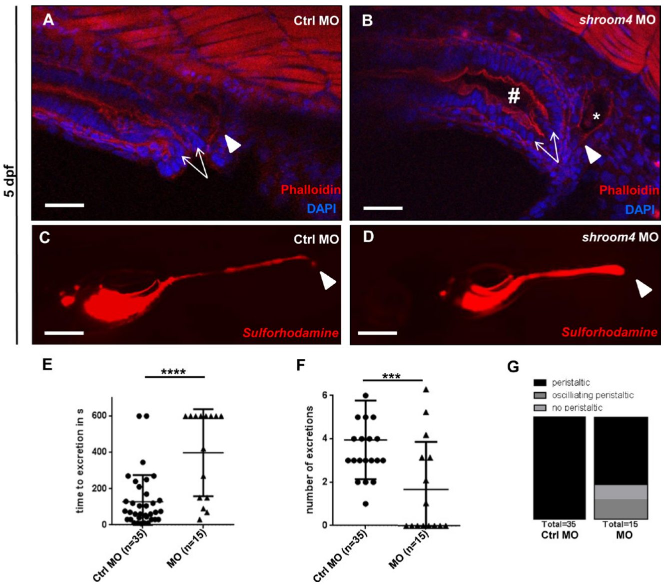

Figure 4 Phalloidin stainings and SR101 excretion assay show cloacal obstruction in *shroom4* morphants. (A,B) Cloacal region is depicted at 5 dpf. White arrows indicate the hindgut; the white arrowheads show the distal pronephric ducts. With *shroom4* MO-injected zfl display a dilated hindgut and distal pronephric morphology compared with Ctrls. (C,D) KD with *shroom4* MO causes an abnormal cloacal excretion of SR101 compared with Ctrl MO-injected zfl at 5 dpf elucidated by white arrowheads (C,D). (E–G) *shroom4* morphants show significantly longer time to excretion (E), significantly reduced number of excretions over time (F), and oscillating or missing peristalsis compared with Ctrls (G) (n=3). Scale bars represent 30 µm (A,B) and 100 µm (C,D). Ctrl, control; MO, morpholino oligonucleotide; SR101, sulforhodamine 101; zfl, zebrafish larvae.

the formation of urinary tract anomalies and the neurodevelopmental disorders in these individuals. Interestingly, microdeletions comprising *CLCN5* and *SHROOM4* have been previously associated with DD, ID, growth retardation, dysmorphic craniofacial features and Dent's disease (online supplemental table S1).[9 10]

The observed phenotypes in *shroom4* MO KD zfl resemble somehow the phenotypical spectrum observed in the affected individuals with genetic *SHROOM4* variations reported here. The KD of Shroom4 led to decreased eye diameter and head size. The observation of a reduced eye-to-head ratio within the morphant zfl suggests a growth-independent effect. This assay has been previously used as a proxy to easily observe effects on neurogenesis, migration and patterning, showing the close relation of eye size and neurodevelopmental disorders in the zebrafish model.[39] Embryonic expression data in mouse embryos and zfl implicate *Shroom4*/*shroom4* in early brain formation, implicating that the observed reduced eye-to-head ratio could represent the neurodevelopmental phenotypes in individuals with Stocco dos Santos syndrome, that is, microcephaly, ID and DD (online supplemental table S1).[6 10] Further phenotypical features of *shroom4* MO morphants show affection of the cardiovascular system displaying PE. However, PE might be a non-specific MO effect also observed in Ctrl zfl. Although MO-induced PE could be rescued by wt *SHROOM4* mRNA coinjection, it remains uncertain if PE following Shroom4 KD resembles the cardiovascular phenotypes of families A and B.[40 41] The formation of the pronephric cysts and dilated ducts in *shroom4* KD zfl is consistent with the observed anomalies of the upper and lower urinary tract in the affected individuals (table 1). These also resemble the bilateral hydronephrosis caused by an anatomical obstruction due to PUV observed in individual II-4 of family D (figures 3 and 4 and table 1). The dilatation of the pronephric ducts in zfl could also be secondary to the mechanical obstruction of the observed cloacal malformation. The phalloidin staining and SR101 assay frequently visualised cloacal opening defects of the hindgut among *shroom4* MO KD zfl, resembling the ARM in the affected individuals (figure 4B,D, table 1). The complete absence or only partial presence of peristalsis could be due to mechanical obstruction or possibly to a malfunction in the visceral nervous system.

The observed phenotypes PE, reduced survival and reduced eye-to-head ratio were significantly rescued by the coinjection of *shroom4* MO and human wt *SHROOM4* mRNA (figure 3B,C,F). These rescue experiments highlight that the observed phenotypes in *shroom4* MO KD zfl, which resemble several phenotypical features of the reported families, are each specifically caused by the depletion of Shroom4 but can be reduced by coinjection of human wt *SHROOM4* mRNA. While coinjection of *shroom4* MO and human wt *SHROOM4* mRNA resulted in a non-significant reduction of glomerular cyst formation, it still underlines the specificity of our KD for Shroom4. Together, the phenotypical changes in *shroom4* MO KD zfl and the observed expression of *Shroom4* in embryonic mouse tissues suggest *SHROOM4* to be implicated in the development of CNS and other principal structures, that are, the urinary tract and the anorectal and cardiovascular systems. Whereas our KD experiments leading to depletion of Shroom4 resemble the genetic situation of the individuals with *SHROOM4* deletions reported here, our data cannot provide evidence beyond all doubts that the missense variant of family A is indeed responsible for the respective phenotype, as we have not directly tested the variant in family A in our MO KD rescue experiments.

Hence, while additional functional studies are warranted investigating the impact of *SHROOM4* SNVs, our study suggests that the developmental role of *SHROOM4* might be beyond its embryonic role in CNS formation, including an additional role in the development of several other organ systems.

Author affiliations
[1]Institute of Anatomy, Medical Faculty, University of Bonn, Bonn, Germany
[2]Department of Pediatrics, Boston Children's Hospital, Harvard Medical School, Boston, Massachusetts, USA
[3]Institute of Human Genetics, Medical Faculty, University of Bonn, Bonn, Germany
[4]Genomic Medicine Center, Children's Mercy Hospital, Kansas City, Missouri, USA
[5]Department of Pediatrics, Faculty of Medical Sciences, Medical University of Silesia in Katowice, Zabrze, Poland
[6]Department of Pediatrics, University of Zielona Góra, Zielona Góra, Poland
[7]Department of Pediatrics, Faculty of Medical Sciences, Medical University of Silesia, Katowice, Poland
[8]Department of Epilepsy Genetics and Personalized Medicine, Danish Epilepsy Centre, Dianalund, Denmark
[9]Institute for Regional Health Services, University of Southern Denmark, Odense, Denmark
[10]Cologne Center for Genomics (CCG), Faculty of Medicine, University Hospital Cologne, University of Cologne, Cologne, Germany
[11]Institute of Human Genetics, Heidelberg University, Heidelberg, Germany
[12]Department of Pediatrics and Adolescent Medicine, Friedrich-Alexander University of Erlangen-Nürnberg, Erlangen, Germany
[13]Research Center On Rare Kidney Diseases (RECORD), University Hospital Erlangen, Erlangen, Germany
[14]Division of Clinical Genetics, Children's Mercy Hospital, Kansas City, Missouri, USA
[15]Medeor Hospital, Department of Genetics, Lodz, Poland
[16]Institute of Cardiovascular Regeneration, Center for Molecular Medicine, Goethe University, Frankfurt am Main, Germany
[17]Georg-Speyer-Haus, Institute for Tumor Biology and Experimental Therapy, Frankfurt am Main, Germany

[18]Division of Neonatology and Pediatric Intensive Care, Department of Pediatrics and Adolescent Medicine, Friedrich-Alexander University of Erlangen-Nürnberg, Erlangen, Germany
[19]Department of Neuropediatrics, University Hospital Bonn, Bonn, Germany

Acknowledgements We thank the participating families and physicians for their contribution. Zebrafish work was supported by Bonn medical faculty zebrafish core facility. *Tg(wt1b:GFP)* zebrafish was provided by Christoph Englert. This study makes use of data generated by the DECIPHER community. A full list of centres which contributed to the generation of the data is available online (https://deciphergenomics.org/about/stats) and via email from contact@deciphergenomics.org. Funding for the DECIPHER project was provided by Wellcome.

Contributors CMK, TF, ÖY, TTL, BO and GCD performed zebrafish experiments. LS, IT, LB, TP, HT, ACH, HMR and GCD performed exome evaluation and variant analysis. IT, MS, MZ, PA, AB, FH and HMR recruited families and gathered clinical data for the study. ACH, MS, MZ, PA and PGn performed the array analysis. KH and UM conducted X-inactivation studies. PGr conducted mouse experiments. BO, HMR and GCD designed and oversaw the entire study and wrote the manuscript with CMK. GCD is responsible for the overall content as guarantor.

Funding CMK was funded by the SciMed BONFOR stipends (O-149.0120 and O-167.0021), by the German Research Foundation (DFG, KO 6579/2-1) (708037-809683, 499462148) and supported by the Biomedical Education Program (BMEP). IT and TP work was made possible by the generous gifts to Children's Mercy Research Institute and Genomic Answers for Kids program at Children's Mercy Kansas City. Data are available online (https://github.com/ChildrensMercyResearchInstitute/GA4K). FH was supported by the National Institutes of Health NIH (DK068306). ACH was funded by the BONFOR grant (O-149.0123) and partially funded by the Else Kröner-Fresenius-Stiftung and the Eva Luise und Horst Köhler Stiftung (project number 2019_KollegSE.04). We are grateful for a German Research Foundation (DFG) equipment grant (INST 1172/37-1 FUGG) to BO for a multiphoton microscope set-up. HR was funded by the German Research Foundation (DFG, RE 1723/4-1) and by the Else-Kröner-Fresenius-Stiftung (EKFS, 2014_A14). G.CD was funded by the BONFOR grant (O-120.0001).

Competing interests None declared.

Patient consent for publication Not applicable.

Ethics approval This study involves human participants and was approved by the ethics committees of the Medical Faculty of the University of Bonn and of the institutions of respective collaborators (Lfd. Nr. 031/19). Participants gave informed consent to participate in the study before taking part.

Provenance and peer review Not commissioned; externally peer reviewed.

Data availability statement Data are available upon reasonable request. All data relevant to the study are included in the article or uploaded as supplementary information. *SHROOM4* variants identified in this study were submitted to ClinVar.

ORCID iDs
Friedhelm Hildebrandt http://orcid.org/0000-0003-3845-3489
Heiko M Reutter http://orcid.org/0000-0002-3591-5265
Gabriel C Dworschak http://orcid.org/0000-0003-0015-6964

REFERENCES

1 Hildebrand JD, Soriano P. Shroom, a PDZ domain-containing actin-binding protein, is required for neural tube morphogenesis in mice. *Cell* 1999;99:485–97.
2 Yoder M, Hildebrand JD. Shroom4 (Kiaa1202) is an actin-associated protein implicated in cytoskeletal organization. *Cell Motil Cytoskeleton* 2007;64:49–63.
3 dos Santos RC, Barretto OC, Nonoyama K, Castro NH, Ferraz OP, Walter-Moura J, Vescio CF, Beçak W. X-linked syndrome: mental retardation, hip luxation, and G6PD variant [Gd(+) Butantan]. *Am J Med Genet* 1991;39:133–6.
4 Stocco dos Santos RC, Castro NHC, Lillia Holmes A, Beçak W, Tackels-Horne D, Lindsey CJ, Lubs HA, Stevenson RE, Schwartz CE, Holmes AL. Stocco DOS Santos X-linked mental retardation syndrome: clinical elucidation and localization to Xp11.3-Xq21.3. *Am J Med Genet A* 2003;118A:255–9.
5 Hagens O, Dubos A, Abidi F, Barbi G, Van Zutven L, Hoeltzenbein M, Tommerup N, Moraine C, Fryns J-P, Chelly J, van Bokhoven H, Gécz J, Dollfus H, Ropers H-H, Schwartz CE, de Cassia Stocco Dos Santos R, Kalscheuer V, Hanauer A. Disruptions of the novel KIAA1202 gene are associated with X-linked mental retardation. *Hum Genet* 2006;118:578–90.
6 Lopes F, Barbosa M, Ameur A, Soares G, de Sá J, Dias AI, Oliveira G, Cabral P, Temudo T, Calado E, Cruz IF, Vieira JP, Oliveira R, Esteves S, Sauer S, Jonasson I, Syvänen A-C, Gyllensten U, Pinto D, Maciel P. Identification of novel genetic causes of Rett syndrome-like phenotypes. *J Med Genet* 2016;53:190–9.
7 Farwell KD, Shahmirzadi L, El-Khechen D, Powis Z, Chao EC, Tippin Davis B, Baxter RM, Zeng W, Mroske C, Parra MC, Gandomi SK, Lu I, Li X, Lu H, Lu H-M, Salvador D, Ruble D, Lao M, Fischbach S, Wen J, Lee S, Elliott A, Dunlop CLM, Tang S. Enhanced utility of family-centered diagnostic exome sequencing with inheritance model-based analysis: results from 500 unselected families with undiagnosed genetic conditions. *Genet Med* 2015;17:578–86.
8 Honda S, Hayashi S, Imoto I, Toyama J, Okazawa H, Nakagawa E, Goto Y-I, Inazawa J. Copy-Number variations on the X chromosome in Japanese patients with mental retardation detected by array-based comparative genomic hybridization analysis. *J Hum Genet* 2010;55:590–9.
9 Armanet N, Metay C, Brisset S, Deschenes G, Pineau D, Petit FM, Di Rocco F, Goossens M, Tachdjian G, Labrune P, Tosca L. Double Xp11.22 deletion including SHROOM4 and CLCN5 associated with severe psychomotor retardation and dent disease. *Mol Cytogenet* 2015;8:8.
10 Danyel M, Suk EK, Raile V, Gellermann J, Knaus A, Horn D. Familial Xp11.22 microdeletion including SHROOM4 and CLCN5 is associated with intellectual disability, short stature, microcephaly and dent disease: a case report. *BMC Med Genomics* 2019;12:6.
11 Nizon M, Andrieux J, Rooryck C, de Blois M-C, Bourel-Ponchel E, Bourgois B, Boute O, David A, Delobel B, Duban-Bedu B, Giuliano F, Goldenberg A, Grotto S, Héron D, Karmous-Benailly H, Keren B, Lacombe D, Lapierre J-M, Le Caignec C, Le Galloudec E, Le Merrer M, Le Moing A-G, Mathieu-Dramard M, Nusbaum S, Pichon O, Pinson L, Raoul O, Rio M, Romana S, Roubertie A, Colleaux L, Turleau C, Vekemans M, Nabbout R, Malan V. Phenotype-Genotype correlations in 17 new patients with an Xp11.23p11.22 microduplication and review of the literature. *Am J Med Genet A* 2015;167A:111–22.
12 Grams SE, Argiropoulos B, Lines M, Chakraborty P, Mcgowan-Jordan J, Geraghty MT, Tsang M, Eswara M, Tezcan K, Adams KL, Linck L, Himes P, Kostiner D, Zand DJ, Stalker H, Driscoll DJ, Huang T, Rosenfeld JA, Li X, Chen E. Genotype-Phenotype characterization in 13 individuals with chromosome Xp11.22 duplications. *Am J Med Genet A* 2016;170A:967–77.
13 Froyen G, Van Esch H, Bauters M, Hollanders K, Frints SGM, Vermeesch JR, Devriendt K, Fryns J-P, Marynen P. Detection of genomic copy number changes in patients with idiopathic mental retardation by high-resolution X-array-CGH: important role for increased gene dosage of *XLMR* genes. *Hum Mutat* 2007;28:1034–42.
14 Isrie M, Froyen G, Devriendt K, de Ravel T, Fryns JP, Vermeesch JR, Van Esch H. Sporadic male patients with intellectual disability: contribution of X-chromosome copy number variants. *Eur J Med Genet* 2012;55:577–85.
15 Dong Z, Chau MHK, Zhang Y, Dai P, Zhu X, Leung TY, Kong X, Kwok YK, Stankiewicz P, Cheung SW, Choy KW. Deciphering the complexity of simple chromosomal insertions by genome sequencing. *Hum Genet* 2021;140:361–80.
16 Routier L, Verny F, Barcia G, Chemaly N, Desguerre I, Colleaux L, Nabbout R. Exome sequencing findings in 27 patients with myoclonic-atonic epilepsy: is there a major genetic factor? *Clin Genet* 2019;96:254–60.
17 Bian W-J, Li Z-J, Wang J, Luo S, Li B-M, Gao L-D, He N, Yi Y-H. *SHROOM4* Variants Are Associated With X-Linked Epilepsy With Features of Generalized Seizures or Generalized Discharges. *Front Mol Neurosci* 2022;15:862480.
18 Heide S, Spentchian M, Valence S, Buratti J, Mach C, Lejeune E, Olin V, Massimello M, Lehalle D, Mouthon L, Whalen S, Faudet A, Mignot C, Garel C, Blondiaux E, Lefebvre M, Quenum-Miraillet G, Chantot-Bastaraud S, Milh M, Bretelle F, Portes Vdes, Guibaud L, Putoux A, Tsatsaris V, Spodenkiewic M, Layet V, Dard R, Mandelbrot L, Guet A, Moutton S, Gorce M, Nizon M, Vincent M, Beneteau C, Rocchisanni M-A, Benachi A, Saada J, Attié-Bitach T, Guilbaud L, Maurice P, Friszer S, Jouannic J-M, de Villemeur TB, Moutard M-L, Keren B, Héron D. Prenatal exome sequencing in 65 fetuses with abnormality of the corpus callosum: contribution to further diagnostic delineation. *Genet Med* 2020;22:1887–91.
19 Hilger A, Schramm C, Draaken M, Mughal SS, Dworschak G, Bartels E, Hoffmann P, Nöthen MM, Reutter H, Ludwig M. Familial occurrence of the VATER/VACTERL association. *Pediatr Surg Int* 2012;28:725–9.
20 Kolvenbach CM, Dworschak GC, Frese S, Japp AS, Schuster P, Wenzlitschke N, Yilmaz Öznur, Lopes FM, Pryalukhin A, Schierbaum L, van der Zanden LFM, Kause F, Schneider R, Taranta-Janusz K, Szczepańska M, Pawlaczyk K, Newman WG, Beaman GM, Stuart HM, Cervellione RM, Feitz WFJ, van Rooij IALM, Schreuder MF, Steffens M, Weber S, Merz WM, Feldkötter M, Hoppe B, Thiele H, Altmüller J, Berg C, Kristiansen G, Ludwig M, Reutter H, Woolf AS, Hildebrandt F, Grote P, Zaniew M, Odermatt B, Hilger AC. Rare

variants in BNC2 are implicated in autosomal-dominant congenital lower urinary-tract obstruction. *Am J Hum Genet* 2019;104:994–1006.
21 Sobreira N, Schiettecatte F, Boehm C, Valle D, Hamosh A. New tools for Mendelian disease gene identification: PhenoDB variant analysis module; and GeneMatcher, a web-based tool for linking Investigators with an interest in the same gene. *Hum Mutat* 2015;36:425–31.
22 Sobreira N, Schiettecatte F, Valle D, Hamosh A. GeneMatcher: a matching tool for connecting Investigators with an interest in the same gene. *Hum Mutat* 2015;36:928–30.
23 Allen RC, Zoghbi HY, Moseley AB, Rosenblatt HM, Belmont JW. Methylation of HpaII and HhaI sites near the polymorphic CAG repeat in the human androgen-receptor gene correlates with X chromosome inactivation. *Am J Hum Genet* 1992;51:1229–39.
24 Chotteau-Lelièvre A, Dollé P, Gofflot F. Expression analysis of murine genes using in situ hybridization with radioactive and nonradioactively labeled RNA probes. *Methods Mol Biol* 2006;326:61–87.
25 Westerfield M. *The zebrafish book. A guide for the laboratory use of zebrafish (Danio rerio)*. Eugene: Univ. of Oregon Press, 2000.
26 Kimmel CB, Ballard WW, Kimmel SR, Ullmann B, Schilling TF. Stages of embryonic development of the zebrafish. *Dev Dyn* 1995;203:253–310.
27 Thisse C, Thisse B. High-Resolution in situ hybridization to whole-mount zebrafish embryos. *Nat Protoc* 2008;3:59–69.
28 Rieke JM, Zhang R, Braun D, Yilmaz Öznur, Japp AS, Lopes FM, Pleschka M, Hilger AC, Schneider S, Newman WG, Beaman GM, Nordenskjöld A, Ebert A-K, Promm M, Rösch WH, Stein R, Hirsch K, Schäfer F-M, Schmiedeke E, Boemers TM, Lacher M, Kluth D, Gosemann J-H, Anderberg M, Barker G, Holmdahl G, Läckgren G, Keene D, Cervellione RM, Giorgio E, Di Grazia M, Feitz WFJ, Marcelis CLM, Van Rooij IALM, Bökenkamp A, Beckers GMA, Keegan CE, Sharma A, Dakal TC, Wittler L, Grote P, Zwink N, Jenetzky E, Brusco A, Thiele H, Ludwig M, Schweizer U, Woolf AS, Odermatt B, Reutter H. *SLC20A1* Is Involved in Urinary Tract and Urorectal Development. *Front Cell Dev Biol* 2020;8.
29 Emerson SE, St Clair RM, Waldron AL, Bruno SR, Duong A, Driscoll HE, Ballif BA, McFarlane S, Ebert AM. Identification of target genes downstream of semaphorin6A/PlexinA2 signaling in zebrafish. *Dev Dyn* 2017;246:539–49.
30 Parkin CA, Allen CE, Ingham PW. Hedgehog signalling is required for cloacal development in the zebrafish embryo. *Int J Dev Biol* 2009;53:45–57.
31 Baranowska Körberg I, Hofmeister W, Markljung E, Cao J, Nilsson D, Ludwig M, Draaken M, Holmdahl G, Barker G, Reutter H, Vukojević V, Clementson Kockum C, Lundin J, Lindstrand A, Nordenskjöld A. Wnt3 involvement in human bladder exstrophy and cloaca development in zebrafish. *Hum Mol Genet* 2015;24:5069–78.
32 Dietz ML, Bernaciak TM, Vendetti F, Kielec JM, Hildebrand JD. Differential actin-dependent localization modulates the evolutionarily conserved activity of Shroom family proteins. *J Biol Chem* 2006;281:20542–54.
33 Firth HV, Richards SM, Bevan AP, Clayton S, Corpas M, Rajan D, Van Vooren S, Moreau Y, Pettett RM, Carter NP. Decipher: database of chromosomal imbalance and phenotype in humans using Ensembl resources. *Am J Hum Genet* 2009;84:524–33.
34 Thisse B, Thisse C. *Fast release clones: a high throughput expression analysis. ZFIN direct data submission*, 2004.
35 Perner B, Englert C, Bollig F. The Wilms tumor genes wt1a and wt1b control different steps during formation of the zebrafish pronephros. *Dev Biol* 2007;309:87–96.
36 Piton A, Redin C, Mandel J-L. XLID-causing mutations and associated genes challenged in light of data from large-scale human exome sequencing. *Am J Hum Genet* 2013;93:368–83.
37 Levtchenko EN, Monnens LAH, Bökenkamp A, Knoers NV. [From gene to disease; Dent's disease caused by abnormalities in the CLCN5 and OCRL1 genes]. *Ned Tijdschr Geneeskd* 2007;151:2377–80.
38 Lieske JC, Milliner DS, Beara-Lasic L. *Dent Disease. GeneReviews® [Internet]*. Seattle, WA: University of Washington, Seattle, 2012: 1993–2021.
39 Novorol C, Burkhardt J, Wood KJ, Iqbal A, Roque C, Coutts N, Almeida AD, He J, Wilkinson CJ, Harris WA. Microcephaly models in the developing zebrafish retinal neuroepithelium point to an underlying defect in metaphase progression. *Open Biol* 2013;3:130065.
40 Hanke N, Staggs L, Schroder P, Litteral J, Fleig S, Kaufeld J, Pauli C, Haller H, Schiffer M. "Zebrafishing" for novel genes relevant to the glomerular filtration barrier. *Biomed Res Int* 2013;2013:1–12.
41 Gee HY, Ashraf S, Wan X, Vega-Warner V, Esteve-Rudd J, Lovric S, Fang H, Hurd TW, Sadowski CE, Allen SJ, Otto EA, Korkmaz E, Washburn J, Levy S, Williams DS, Bakkaloglu SA, Zolotnitskaya A, Ozaltin F, Zhou W, Hildebrandt F. Mutations in EMP2 cause childhood-onset nephrotic syndrome. *Am J Hum Genet* 2014;94:884–90.

Table S1. Summary of genetic and clinical features in individuals with *SHROOM4* variations

Variation type	Genetic change	Neurocognitive/developmental phenotype	Other manifestations	Reference
SNV: missense	NM_020717.4: c.3266C>T; p.(S1089L)	four-generation pedigree with multiple affected members: severe ID, delayed or no speech, seizures, periods of depression, aggressiveness and hyperactivity, short stature	bilateral congenital hip luxation, scoliosis	Stocco dos Santos et al. [3-4], Hagens et al. [5]
	NM_020717.4: c.436C>T; p.(R146W)	dyspraxic gait, speech delay, eye pointing, peripheral vasomotor disturbances, microcephaly	kyphosis, small cold hand and feet	Lopes et al. [6]
	NM_020717.4: c.1913C>G; p.(S638C)	Stocco dos Santos syndrome		Farwell et al. [7]
	NM_020717.4: c.1201C>T; p.(H401Y)	myoclonic atonic epilepsy		Routier et al. [16]
	NM_020717.4: c.13C>A; p.(P5T), c.3236C>T; p.(E1079A), c.3581C>T; p.(S1194L), c.4288C>T; p.(R1430C), c.4303G>A;p.(V1435M), c.4331C>T; p.(P1444L)	six unrelated male individuals with idiopathic epilepsy		Bian et al. [17]
SNV: nonsense	NM_020717.4: c. 2050C>T; p.(R684*)	complete corpus callosum agenesis, Blake’s pouch cyst	Turner syndrome	Heide et al. [18]
Structural: deletions	Xp11.23p11.22; 2.86 Mb	mild ID		Honda et al. [8]
	Xp11.22; 0.14 Mb and 2.6 Mb	hydrocephalus, severe growth and psychomotor retardation	Dent's disease: renal proximal tubulopathy with low-molecular-weight proteinuria, hypercalciuria, hyperaminoaciduria, hypophosphatemia and hyperuricemia	Armanet et al. [9]
	Xp11.23p.11.22; 0.7 Mb	mild ID, speech delay, microcephaly, short stature, developmental delay	short fingers with bilateral clinodactyly V, short toes, Dent's disease: proteinuria, nephrocalcinosis and	Danyel et al. [10]

			hypophosphatemia, facial dysmorphology	
Structural: duplications	Xp11.23p11.22; 4.4 - 8.9 Mb	12 affected individuals: 12/12 mild-severe ID, 12/12 language impairment, 11/12 psychomotor delay, 8/12 behavious disorder (autism, aggressiveness, hyperactivity), 7/12 sleeping disorder, 6/12 epilepsy, 5/12 hypotonia, 4/12 abnormal brain MRI	5/12 extremity abnormalities, 7/12 early onset of puberty, 1/12 shawl scrotum	Nizon et al. [11]
	Xp11.23p11.22; 0.34 - 4.6 Mb	9 affected individuals: 9/9 mild to severe ID, 8/9 speech delay, 7/9 attention deficit disorder, 7/9 motor delay, 4/9 autism	6/9 hand abnormalities (clinodactyly V and/or tapering fingers), 6/9 foot abnormalities, 4/5 early onset of menses in females, 5/9 synophrys, 5/9 constipation	Grams et al. [12]
	Xp11.23 3.1 Mb	developmental delay, stereotypic movements, poor communication, autistic features	broad thorax, wide-spaced nipples	Froyen et al. [13]
	Xp11.22; 0.26 Mb (possibly disrupting *SHROOM4* locus)	developmental delay	choanal atresia, ventricle septum defect and camptodactyly	Isrie et al. [14]
Structural: complex rearrangements	individual 1: 46,X,t(X;8)(p11.2;p22.3); individual 2: 46,X,t(X;19)(p11.2;p13.3)	two female individuals with mild to moderate ID (2/2) individual 1: seizures, aggressive behavior, delayed motor skills, normal brain MRI. individual 2: intrauterine growth delay, short stature, hypotrophic limbs	individual 1: mild hyperextensibility of fingers, mild clinodactyly V, cutaneous syndactyly II/III individual 2: foot abnormalities, both individuals: discrete facial dysmorphology individual 2: right cardiac ventricular dysplasia of unknown origin	Hagens et al. [5]
	dup(X)(p11.22p11.21); 4.6 Mb duplication and insertion	moderate developmental delay, autism spectrum disorder		Dong et al. [15]

SUPPLEMENTAL DATA

Supplemental note

Clinical Report of Family A: In Family A, the index individual (III-1) and her maternal uncle (II-3) showed several CFs of the VATER/VACTERL association: Individual III-1 presented with anorectal malformation (A; vestibular fistula), tetralogy of Fallot (C), esophageal atresia with tracheo-esophageal fistula (TE; Vogt type 3b), and unilateral renal agenesis (R). Her uncle (II-3) showed anorectal malformation (A), esophageal atresia with tracheo-esophageal fistula (TE; Vogt type 3b), unilateral renal agenesis (R), and aplasia of the right radial bone and pre-axial polydactyly of the left hand (L). Both individuals showed normal physical and neurocognitive development. At the time of assessment, the index individual was a student of good standing in high school and her uncle had a degree from university. Ultrasound examinations of I-1, I-2, II-2 and III-2 confirmed that these family members were unaffected regarding their internal organ status.

Supplemental figures and tables

Figure S1. Results of molecular karyotyping in individuals II-2 and II-1 (Family C)

(A) Chromosome Xp11.23p11.22 deletions of 1.07 Mb spanning chrX:g.49,375,617-50,447,320 involving eight genes and six microRNAs is depicted in Genome Studio.

(B) The respective genomic segment is aligned to RefSeq genes (according to hg19)

Figure S2. Exon structure of zebrafish *shroom4* with Morpholino targets.

(A) Schematic depiction of *shroom4* gene with transcripts *shroom4-201* and *shroom4-202* and targets of MO. The *shroom4* MO is overlapping the exon (E) 2 splice donor site.

Kolvenbach CM, *et al. J Med Genet* 2022;0:1–10. doi: 10.1136/jmg-2022-108738

(B) RT-PCR amplified cDNA and Sanger sequencing showed excision of E2 for *shroom4-201* and insertion of 41 base pairs (bp) from intron (I) 2 for *shroom4-202*.

(C) Pictures of ethidium-bromide-stained gel after performing RT-PCR with zfl harvested at 2 dpf for MO and Ctrl MO. MO injected zfl show a weaker band at 397 bp and excision of E2 for *shroom-201*. For *shroom4-202* a weaker band can be seen at 255 bp and the insertion of 41 intronic bp is shown. *eef1α1* is used as a housekeeping gene control indicating an equal expression of *eef1α1* in both samples.

Table S1. Summary of genetic and clinical features in individuals with *SHROOM4* variations

This supplementary table depicts the genetic and clinical features of previously described affected individuals. The table is divided in two subgroups: single nucleotide variants (SNV), comprising missense and nonsense variants, and structural variations, including deletions, duplications and complex rearrangements. Abbreviations are as follows: ID, intellectual disability; MRI, Magnetic resonance imaging

Kolvenbach CM, *et al. J Med Genet* 2022;0:1–10. doi: 10.1136/jmg-2022-108738

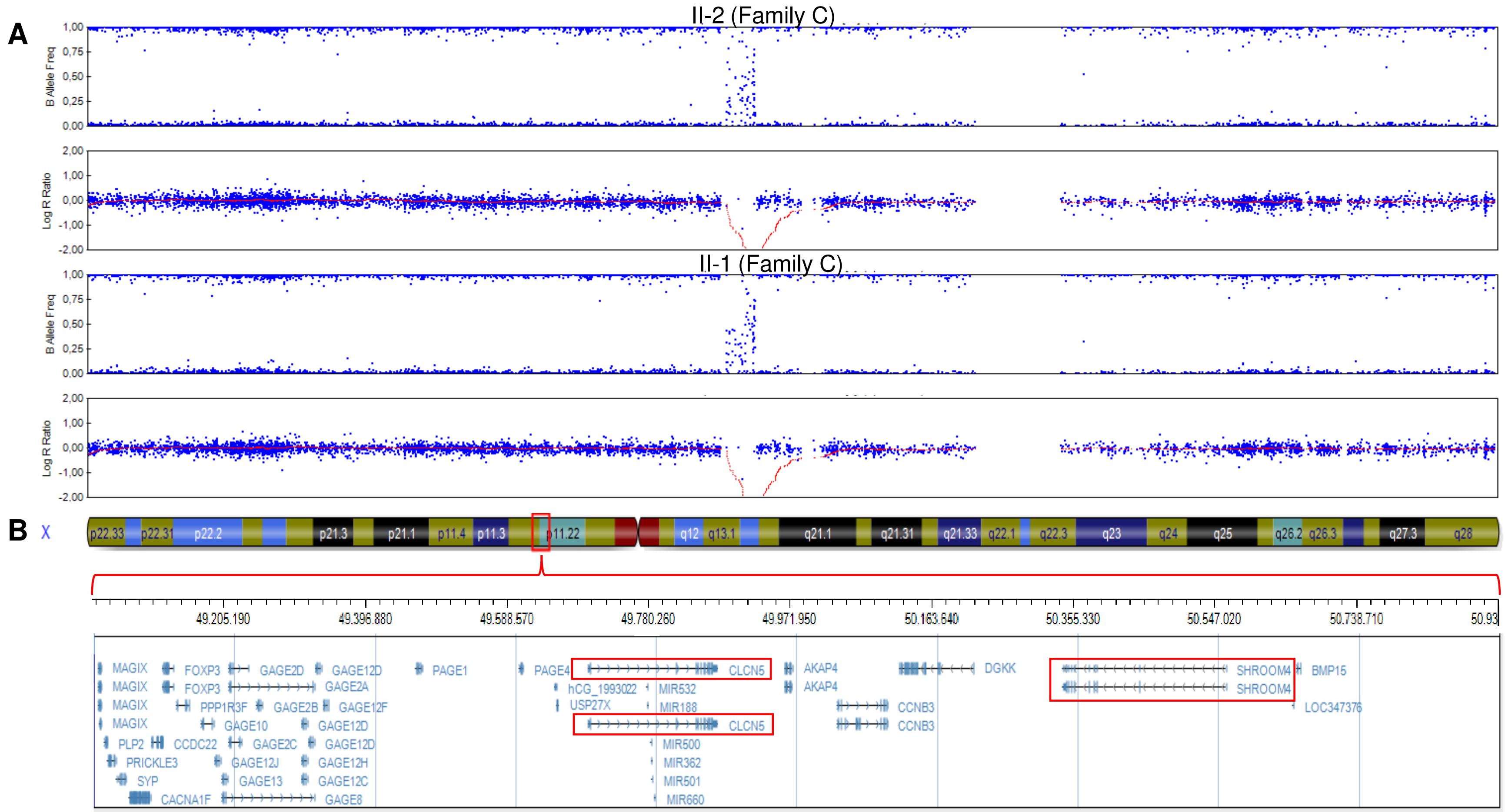
A
II-2 (Family C)
B Allele Freq
Log R Ratio
II-1 (Family C)
B
X
CLCN5
SHROOM4

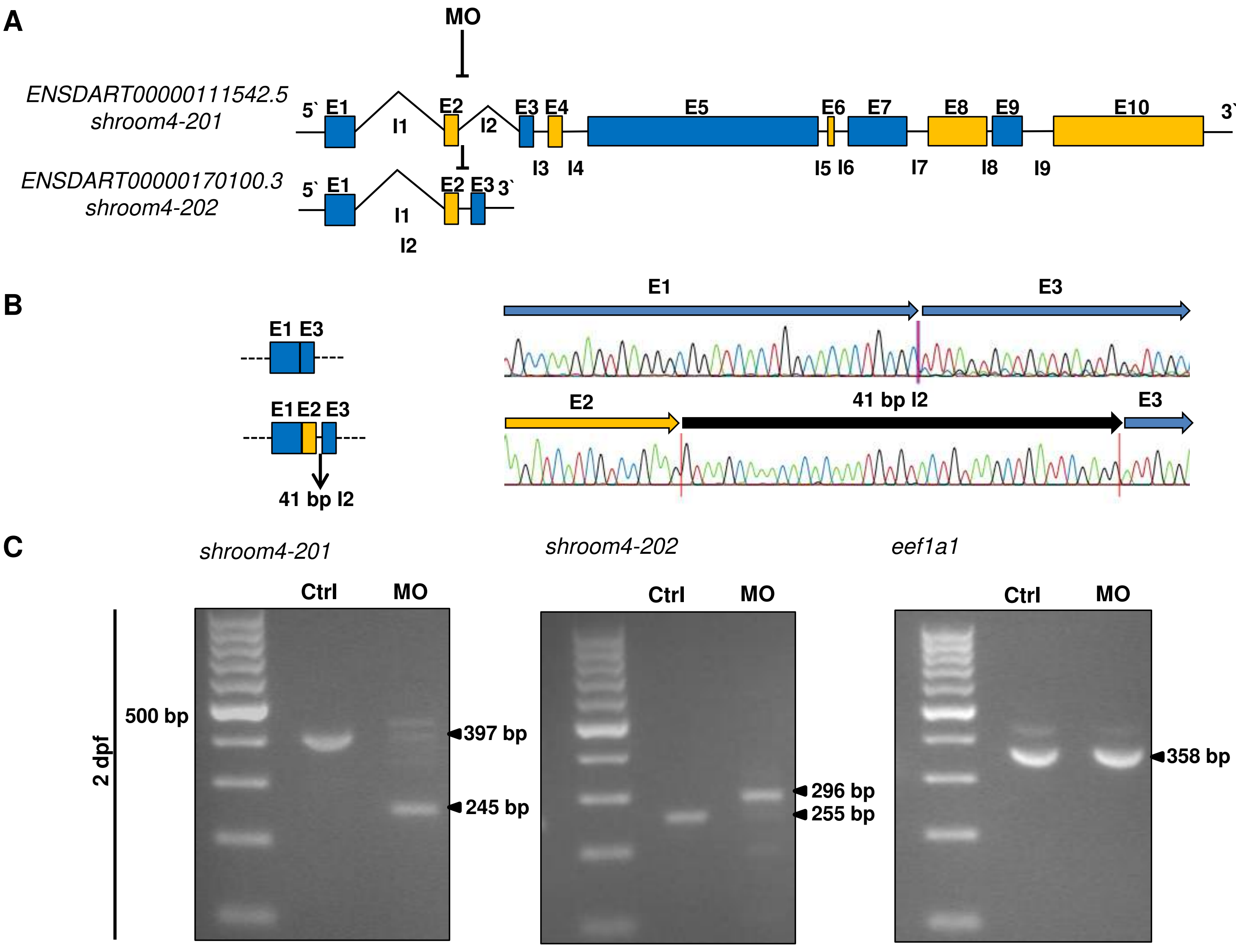
A
MO
ENSDART00000111542.5
shroom4-201
5`
E1
I1
E2
I2
E3
E4
E5
E6
E7
E8
E9
E10
3`
I3
I4
I5
I6
I7
I8
I9
ENSDART00000170100.3
shroom4-202
5`
E1
I1
E2
E3
3`
I2
B
E1
E3
E1
E3
E1
E2
E3
41 bp I2
E2
41 bp I2
E3
C
shroom4-201
shroom4-202
eef1a1
Ctrl
MO
Ctrl
MO
Ctrl
MO
2 dpf
500 bp
397 bp
245 bp
296 bp
255 bp
358 bp